Science of the Total Environment 771 (2021) 144800

Contents lists available at ScienceDirect

Science of the Total Environment

journal homepage: www.elsevier.com/locate/scitotenv

Effective removal of ammonium nitrogen using titanate adsorbent: Capacity evaluation focusing on cation exchange

Wenlong Zhang, Zhenyu Wang, Yunpeng Liu, Jiangtao Feng *, Jie Han, Wei Yan

Department of Environmental Science and Engineering, State Key Laboratory of Multiphase Flow in Power Engineering, School of Energy and Power Engineering, Xi'an Jiaotong University, Xi'an 710049, China

HIGHLIGHTS

- Cation exchange was focused to enhance the adsorption performance of titanate.
- Five amorphous titanates were facilely synthesized for NH_4^+ removal from water.
- The adsorption performance of as-prepared titanates was counter cations dependent.
- The ion selectivity of cations to titanates framework was affected by ions property.
- Affinity coefficient K_f is defined to indicate the cation exchange process.

GRAPHICAL ABSTRACT

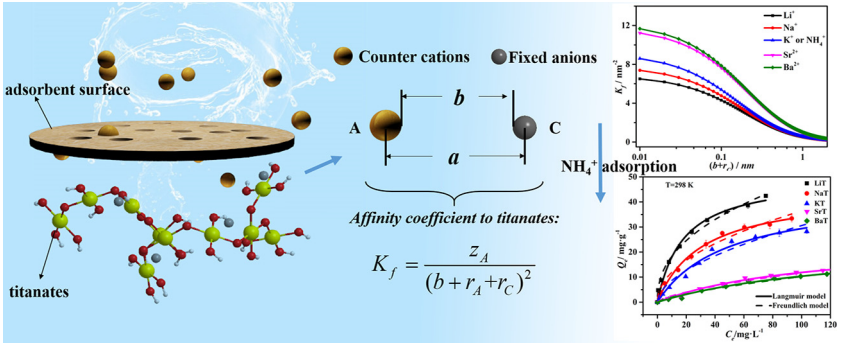

ARTICLE INFO

Article history:
Received 26 September 2020
Received in revised form 19 December 2020
Accepted 19 December 2020
Available online 27 January 2021

Editor: Jay Gan

Keywords:
Ammonium nitrogen
Cation exchange
Titanates
Ion selectivity
Affinity coefficient

ABSTRACT

Cation exchange is one of the dominant mechanisms in the adsorption of cationic ammonium nitrogen (NH_4^+) from water. In this study, we focus on the role of counter cations in cation exchange process of NH_4^+ to enhance the adsorption capacity. Five amorphous titanates namely lithium titanate (LiT), sodium titanate (NaT), potassium titanate (KT), strontium titanate (SrT) and barium titanate (BaT) with different counter cation were facilely synthesized. The adsorption performance for NH_4^+ by these samples is in the order of LiT> NaT > KT> > SrT > BaT. The maximum adsorption capacity of LiT calculated by Langmuir is as high as 50.31 $mg \cdot g^{-1}$. According to the experimental results and theoretical analysis, the electrostatic interaction between counter ions (cations in framework or eternal solution) and charged framework (fixed ions) is the main influence factor during cation exchange process in general. The cation valence and the hydrated ionic radius of the counter ions can inversely affect the ion exchange equilibrium and the affinity of counter ions to titanates. Therefore, a definition of a brief parameter, affinity coefficient K_f (relating to ion valence and distance between opposite charged ions), is introduced and used to explain the difference in adsorption performance of five titanates for NH_4^+. The conclusion about cation exchange and ions affinity may provide possible strategies for enhancement of cationic contaminant adsorption from water or wastewater.

1. Introduction

During the past decades, ammonium nitrogen (NH_4^+) removal has drawn much attention in water treatment research area due to its excessive contents in waterbody (Kelly and He, 2014), which tends to bring a series of environmental issues like eutrophication (Yang et al.,

* Corresponding author.
E-mail address: fjtes@xjtu.edu.cn (J. Feng).

https://doi.org/10.1016/j.scitotenv.2020.144800
0048-9697/

2016). Adsorption, one of the typical and developed water treatment methods, has been widely investigated in the uptake of NH_4^+ from wastewater because of its straightforward process and high efficiency (Adam et al., 2019b). A few common materials including zeolite (Adam et al., 2019a; Vocciante et al., 2018), hydrogel (Zheng and Wang, 2015), resin (Chen et al., 2019) and biochar (Vu et al., 2017) were used to adsorb NH_4^+. Numerous literatures revealed that ion exchange is the main adsorption route for NH_4^+ uptake instead of physical or chemical adsorption (Abukhadra and Mostafa, 2019). There were several methods created to enhance the adsorption capacity of samples for NH_4^+ but few of them focused on the cation exchange process.

It has been deduced that some properties like surface area, size of the adsorbents and surface chemistry could affect cation exchange performance of adsorbent materials for the removal of cationic chemicals (He et al., 2017; Wang et al., 2019). Among these factors, the effect of counter ions (original cations in the adsorbent framework which can be exchanged) plays an important role due to its significant impact on the ion exchange performance proved by experimental results (O'Connor et al., 2020).

Understanding the cation exchange process in NH_4^+ adsorption is in favor of mechanism analysis and adsorbent material design. The equilibrium between cation exchangers and solution has been frequently investigated by a sum of experimental and theoretical approaches. Some of the initial theoretical works only described the equilibria state by empirical equations and the theories developed later were in consistent with experimental results (Kamcev et al., 2016; Kamcev et al., 2017; Katchalsky et al., 1953; Lazare et al., 1956). According to these theories and models, the counter cations play a key role in determining the cation exchange equilibrium and further the adsorption performance (Chen et al., 2018). However, up to now, the effect of counter cations on the ion exchange of NH_4^+ by adsorbent materials from water is still unclear. It is widely observed that materials containing certain amount of Na^+ like zeolite performs well in the adsorption of NH_4^+, which also inspires the modification of adsorbents with Na compounds. However, it is rarely discussed about the synthesis and application of other cations (like Li^+, K^+) contained adsorbents for the NH_4^+ wastewater treatment, especially about the correlation between ion exchange performance and counter ions properties.

Although the theoretical knowledge on ion exchange equilibrium is generally precise now, it is still difficult to briefly describe a certain practical cation exchange process by the complex equations or models because most of the parameters hereon are arduously obtained like swelling pressure of materials (Helfferich, 1962). Only the qualitative discussion of counter ions and ion exchange equilibrium was employed in the application (Hu et al., 2020; Li et al., 2012), which might not be enough for analysis. For example, the ionic radius and valence are considered to have opposite effect on the ion exchange equilibrium. These two parameters of Na^+ are both different from that of Ca^{2+}, which might easily make confusions when used to analyze the cation exchange performance. Therefore, a brief but effective equation or parameter is necessary for the analysis of effect of counter ions on cation exchange process.

Titanate, one of typical cation exchange materials that have been widely used in water purification (Yang et al., 2013), can be facilely prepared with different counter cations and be appropriate for cationic contaminant removal. Therefore, there are several issues discussed in this article: 1) A series of titanates with different counter ions were facilely synthesized and characterized; 2) The performance of these titanates for NH_4^+ removal from simulated wastewater were investigated and compared; 3) The effect of counter ions on NH_4^+ removal was investigated through competitive experiment and theoretical discussion of the selectivity; 4) A new parameter, affinity coefficient K_f, was introduced for more powerful explanation and indication.

2. Experimental procedures

2.1. Chemicals

Titanium isopropoxide ($(Ti(OC_3H_7)_4$, TIPT), isopropanol (99.7%), lithium hydroxide (LiOH), potassium hydroxide (KOH), strontium hydroxide ($Sr(OH)_2$), sodium hydroxide (NaOH) and barium hydroxide ($Ba(OH)_2 \cdot 8H_2O$) were of analytical reagent grade and purchased from Sinopharm Chemical Reagent Co., Ltd., China without purification. The simulated wastewater (1000 $mg \cdot L^{-1}$ of NH_4^+) obtained by dissolving ammonium chloride (NH_4Cl, Guaranteed reagent) into deionized water was stocked for use. The deionized water was obtained by EPED-40TF Superpure Water System.

2.2. Synthesis of titanate samples

Five titanate samples were prepared according to a previous reported hydrolysis method (Zhang et al., 2019). During the synthesis, 10 mL TIPT was added to 4 mL isopropanol to form a homogeneous solution, the mixture was then added into 200 mL 0.1 $mol \cdot L^{-1}$ LiOH solution with magnetic agitation at 60 °C for 2 h. Afterwards, the above mixed solution was agitated for another half an hour at room temperature. The final white suspension was filtrated and the solid from the filtration was rinsed with deionized water for various times until the pH value of filtrate was about 7.0. After that, the solid was dried at 60 °C in an oven for 12 h. The other alkaline solution, 0.1 $mol \cdot L^{-1}$ NaOH, 0.1 $mol \cdot L^{-1}$ KOH, a mixture of NaOH and $Ba(OH)_2$ (0.05 $mol \cdot L^{-1}$ for both two components), a mixture of NaOH and $Sr(OH)_2$ (0.05 $mol \cdot L^{-1}$ for both two components) replaced 0.1 $mol \cdot L^{-1}$ LiOH for the preparation of other titanates, $Sr(OH)_2$ or $Ba(OH)_2$ was added with NaOH on account of their weak solubility. The as-prepared titanates were denoted as LiT (lithium titanate), NaT (sodium titanate), KT (potassium titanate), SrT (strontium titanate), BaT (barium titanate) according to the counter ions, respectively.

2.3. Samples characterization

The morphology of the titanate samples was investigated using a scanning electron microscopy (SEM, MAIA3 LMH, USA). The surface elements distribution of the materials was determined by the energy dispersive X-ray spectrometry (EDX, Gemini 500, Zeiss, Germany). Powder X-ray diffraction (XRD, Bruker, Germany) was used to analyze the crystallographic phases of adsorbents. The X-ray Fluorescence Spectrometer (XRF, S4PIONEER, Germany) and X-ray photoelectron spectroscopy (XPS, AXIS ULtrabld, UK) were used to know the composition of samples. The functional groups of adsorbent materials were tested by a fourier transform infrared spectrometer (FT-IR, Bruker, Germany). The Brunauer-Emmett-Teller specific surface area (S_{BET}) was determined on the Builder SSA-4300 analyzer (Beijing, China). The zeta potential of the samples was measured with Brookhaven 90plus Zeta, samples of which (1.0 mg) were added into 10 mL NaCl solution (10^{-3} $mol \cdot L^{-1}$) at different pH values.

The NH_4^+ concentration of solution before and after adsorption was measured by the salicylate spectrophotometric method (Lovibond, Germany). The concentration of Li^+, Na^+, K^+, Ca^{2+} and Mg^{2+} in water were obtained with the help of ion chromatograph (DiONEX INTEGRION, USA). The concentration of heavy metal ions in the aqueous solution after competitive adsorption were measured by inductively coupled plasma emission spectrometer (ICPE-9000, Japan).

2.4. Adsorption experiments

The batch experiments were mainly performed at 25 °C. The final suspensions were filtrated with 0.45 μm acetate membrane filter for further measurement of the concentration. The adsorption experiments were repeated three times to ensure the reliability of results.

The batch adsorption experiments were studied as follows: The effect of contact time on the adsorption performance was carried out in a beaker with magnetic stirring in water bath by adding 0.2 g of titanates into 100 mL NH_4^+ solution (20 mg·L^{-1}) at 25 °C. About 2 mL solution was withdrawn for further measurement from beaker along with time. To investigate the effect of the solution pH on the adsorption performance, 0.04 g of as-prepared titanate was mixed with 20 mL NH_4^+ solution (20 mg·L^{-1}) at a series of pH values from 2.0–12.0 (modified by NaOH or HCl) in 50 mL centrifugal tube and shook for 120 min in a temperature controlled shaker. Adsorption isotherms for removal of NH_4^+ was performed at the following conditions: 0.04 g of each titanates was added into a 50 mL centrifuge tube, which contained 20 mL adsorbates solution with different initial NH_4^+ concentration varying from 10 to 160 mg·L^{-1}. The mixture was shaken for 120 min in a temperature controlled shaker. The concentration of counter cations in solution after adsorption was also determined to prove the ion exchange process.

The competitive adsorption experiment was conducted as the following procedure: 0.04 g of LT was added into 20 mL mixed solution containing 4.0 meq·L^{-1} NH_4^+ and 1.0, 2.0, 4.0, 6.0, or 8.0 meq·L^{-1} one of the individual coexisting cations, respectively. The cations used in the experiments consist of monovalent cation (Na^+, K^+), divalent cation (Ca^{2+}, Mg^{2+}, Cu^{2+}, Pb^{2+}, Ni^{2+}, Zn^{2+}, Cd^{2+}, Sr^{2+}, Ba^{2+}) and trivalent ion (Al^{3+}, La^{3+}). The initial solution pH was controlled at 3.5 to eliminate the possible effect of precipitate reaction and the contact time was set as 120 min.

The removal rate η (%), the adsorption capacity of as-prepared titanates Q_t (mg·g^{-1}) at time t (min) and Q_e (mg·g^{-1} or meq·g^{-1}) at equilibrium were calculated by Eqs. (1)–(3). Where C_0 (mg·L^{-1} or meq·L^{-1}) is the initial concentration of adsorbates solution, C_t (mg·L^{-1}) and C_e (mg·L^{-1} or meq·L^{-1}) are the concentration of adsorbates solution at time t (min) and equilibrium; m (g) is the adsorbent mass and V (L) is the initial volume of solution. The unit milligram equivalent was used for the comparison of competitive ion exchange capacity of different cations. As shown in Eqs. (S1)–(S4), kinetic models (pseudo-first order and pseudo-second order models) and isotherm models (Langmuir and Freundlich models) were used to analyze the adsorption data and reveal the adsorption process.

$$\eta = \frac{C_0 - C_t}{C_0} \times 100 \tag{1}$$

$$Q_t = \frac{C_0 - C_t}{m} \times V \tag{2}$$

$$Q_e = \frac{C_0 - C_e}{m} \times V \tag{3}$$

3. Results and discussion

3.1. Characteristics

The SEM images presented in Fig. 1 clearly shows the particle morphologies of the titanates. All the titanate samples possess same morphology indicating that ion species used in synthesis is irrelative to the micro-structure formation. However, the particles sizes of these samples varied along with different ion species. According to Fig. 1(a–c) and (d–e), agglomeration occurs more frequently in SrT and BaT than LiT, NaT and KT. The BET surface area ($m^2 \cdot g^{-1}$) and pore volume ($cm^3 \cdot g^{-1}$) of these samples are listed in Table 1 (Fig. S1 shows N_2 gas adsorption-desorption isotherm). It's shown that the surface areas of SrT and BaT are significantly larger than those of LiT, NaT and KT, which is correlated to the decrease of particles size. From the inset in Fig. S1, the SrT and BaT are predominantly microporous and LiT, NaT and KT are mainly mesoporous, which is constant with the average pore diameter value in Table 1. The surface area of titanates in this study can be controlled from around 20 to 200 $m^2 \cdot g^{-1}$ via changing counter ion species. The change of interaction between different counter cations and framework might cause the above phenomenon. In addition, the XRD results (Fig. S2) indicate that all the titanate materials are amorphous except that SrT possesses weak crystalline, which is consistent with the results of hydrolysis process in literatures (di Bitonto et al., 2017; Li et al., 2013).

It is well accepted that the existence of counter cations is related to the adsorption performance of titanates (Zhao et al., 2019). The XRF result (Table 1) successfully demonstrates that Na^+, K^+, Sr^{2+} and Ba^{2+} were introduced to the titanate framework during the synthesis process. The XPS result (Fig. S3) made it clear that Li^+ entered into LiT after the synthesis. The element distribution on the surface of each titanate was measured by the EDX mapping and the results are shown in Fig. S4. It is obvious that Ti, O and metal ions are uniformly distributed on the surface of titanates. It's worth noting that there is little Na^+ contained in as-prepared SrT and BaT although NaOH was used in the synthesis procedure, which indicated that the interactions between Sr^{2+} or Ba^{2+} and titanate framework are stronger than that between Na^+ and the framework. Sr^{2+} or Ba^{2+} is preferential to the titanate framework.

The difference of counter ions might also affect the group or bond species in titanates. It is evident from the FTIR spectra of titanates that peaks change or shift are counter ion species dependent (Fig. S5). All the samples exhibit obvious broad peaks at 500 to 700 cm^{-1}, which represents the Ti-O-Ti vibration. The peaks at 1640 cm^{-1} in all samples can be ascribed to O—H bending vibration. The peak at about 1340 cm^{-1} corresponds to the Ti—O bond (Zhang et al., 2017), which has been demonstrated probably owing to the fracture of Ti-O-H by alkali environment. During the hydrolysis process, counter ions entered the structure of titanates and developed interactions (probably ionic bond) with Ti—O bonds (Chen et al., 2010; Ye et al., 2013). The species and amounts of counter cations vary among titanates and contribute to the peak shifting and strength changing of the Ti—O bond in the spectra. In addition, Sr^{2+} and Ba^{2+} differ from alkali metals in chemical properties and can develop covalent bonds with oxygen, which results in the appearance of Sr—O (1477 cm^{-1}) and Ba—O (1512 cm^{-1}) bonds in SrT and BaT, respectively (Khollam et al., 2005; Sadeghzadeh et al., 2017). The above results indicate that the interactions between titanate frameworks and the counter ions are ion species dependent, which is consistent with the XRF results.

The counter cations species also have impact on the surface charge distribution of the as-prepared titanates (Fig. S6). During the synthesis process, the negative charge framework of titanates was compensated by the cations (Li^+, Na^+, K^+, Ba^{2+}, Sr^{2+}) accompanied by the adsorption of electrolyte ions like OH^-, which can affect the charge case of surface (He et al., 2017; Helfferich, 1962). Furthermore, the affinity of cations to titanates vary with the counter ion species, which results in the difference of cations amount in titanates. The electrostatic attraction between the negative charged surface and positive NH_4^+ are beneficial for the actual adsorption process.

3.2. Adsorption kinetics

All the five titanate samples (LiT, NaT, KT, SrT and BaT) were used in the kinetic experiment. The adsorption capacity of NH_4^+ onto these adsorbents are in the order of LiT> NaT > KT > SrT > BaT (Fig. 2a). For the solution with initial concentration of 20 mg·L^{-1}, LiT maintains a high adsorption efficiency (80%) for NH_4^+. The change of counter cations can successfully enhance the adsorption performance of titanates. The adsorption capacity of LiT (Li^+ contained) is 5 times higher than that of BaT (Ba^{2+} contained). It is satisfactory that all the materials can reach adsorption equilibrium within 10 min. The rapid adsorption can be attributed to the nanoscale of particles size and the negative charged surface or framework of materials.

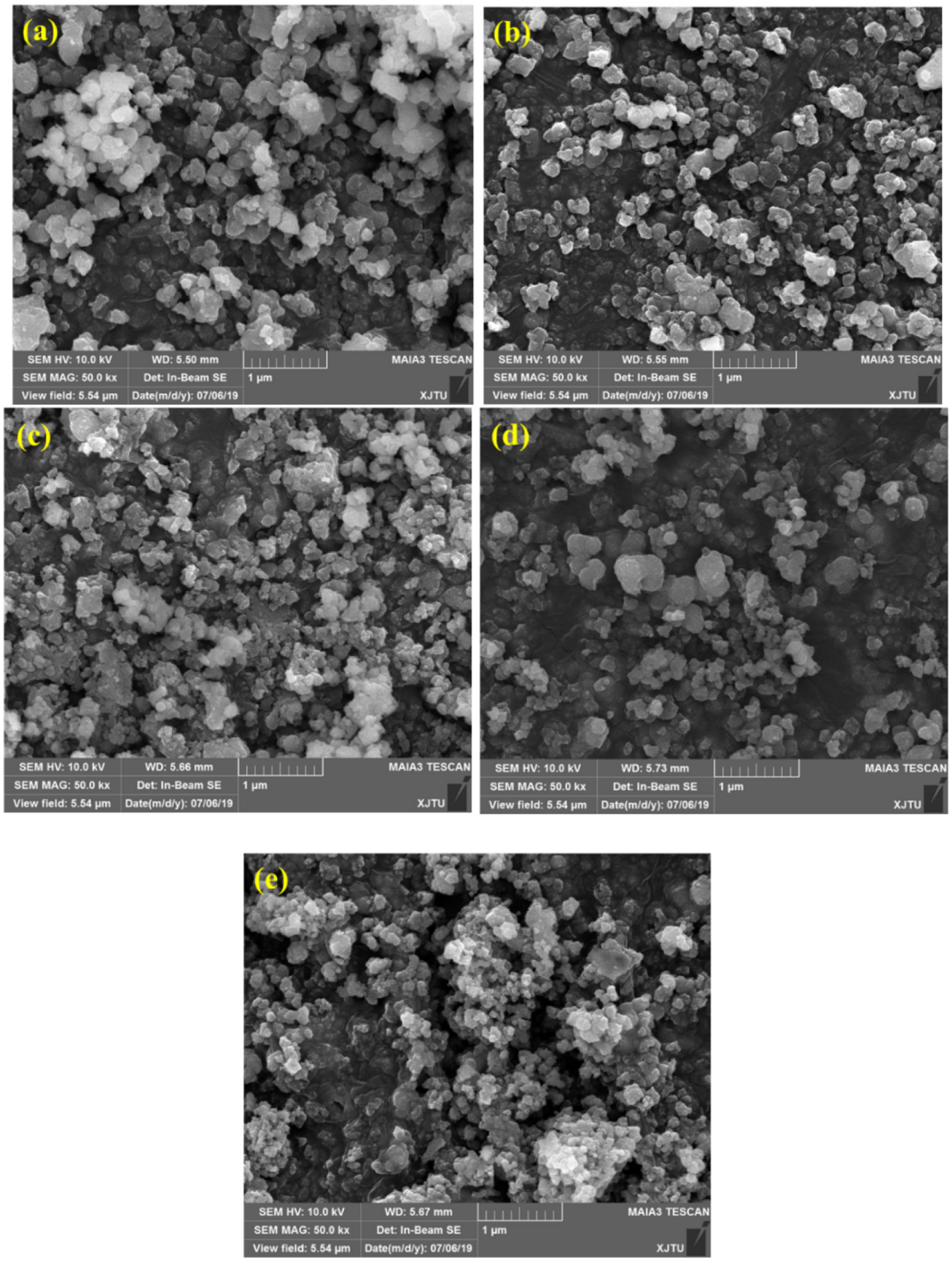

Fig. 1. SEM images of LiT (a), NaT (b), KT (c), SrT (d) and BaT (e).

Furthermore, two typical fitting models (Eqs. (S1)–(S2)) are used to fit the experimental data to reveal the kinetic controlling mode of NH_4^+ onto titanates (Fig. 2a). The calculated results are listed in Table S1. It is clear from the value of R^2 that both pseudo-first-order and pseudo-second-order models fit the experimental data of NaT and BaT well. The adsorption process of NH_4^+ onto LiT and KT can be more effectively revealed by pseudo-second-order model, but the adsorption process for SrT fits the pseudo-first-order model preferably.

Table 1
Physical-chemical properties of titanates by BET and XRF.

Sample	Ti/wt%	O/wt%	Ion/meq·g^{-1}	S_{BET}/m^2·g^{-1}	V/cm^3·g^{-1}	r/nm
LiT	70.8	27.1	Li[a]: 3.13	24.9	0.16	13.3
NaT	64.3	28.4	Na: 3.17	21.9	0.20	12.1
KT	42.7	44.0	K: 3.23	18.5	0.15	15.7
SrT	37.0	47.0	Sr: 3.24 Na:0.300	108.4	0.40	7.40
BaT	31.7	39.5	Ba: 3.90 Na:0.150	207.6	0.46	4.40

[a] The amount of Li^+ was determined by ion chromatography.

3.3. Effect of pH on NH_4^+ adsorption

As a rule, the solution pH has a significant effect on the adsorption performance because the surface state of adsorbent and the form of adsorbate might be pH dependent. For the removal of NH_4^+ from water, the solution pH can effectively influence the form of NH_4^+ (pK_a

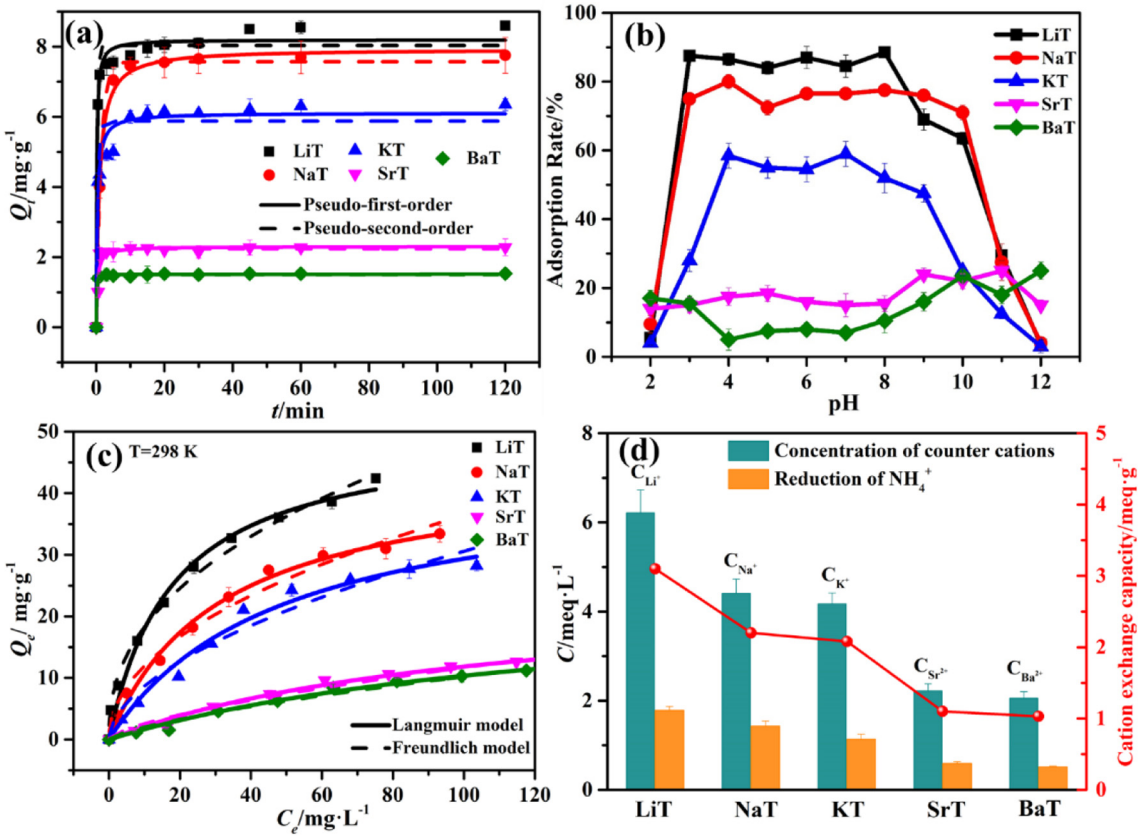

Fig. 2. The evaluation of adsorption performance of titanates. (a) effect of contact time on the adsorption of NH_4^+ by titanates, (b) effect of initial solution pH on the adsorption performance of titanates, (c) adsorption isotherms of NH_4^+ onto the titanates at 25 °C, (d) the cation exchange capacity of titanates, the concentration of counter cations and reduction of NH_4^+ after adsorption of NH_4^+ onto individual titanate. Experimental conditions for (a): initial solution pH = 7, C_0 = 20 mg·L^{-1}; (b): C_0 = 20 mg·L^{-1}, contact time = 120 min; (c): C_0 = 10–160 mg·L^{-1}, solution pH = 7.0, contact time = 120 min; (d): pH = 3.5, C_0 = 40 mg·L^{-1}.

(NH_4^+) = 9.246). As shown in Fig. 2b, the adsorption efficiency of LiT, NaT and KT climb up along with pH and maintain an almost constant value in the pH range of 3.0–9.0 or 4.0–9.0. However, the adsorption of SrT and BaT don't show the same trend, but stay in low level in the whole pH range. In the solution with pH ranging of 3.0–9.0, NH_4^+ is the primary form of ammonium nitrogen (Huang et al., 2008), which is the main component participating the ion exchange with counter ions in titanates. Moreover, the surface of titanates is easily negative charged and attractive for cationic ions in these pH values because of the zeta potential results (Fig. S6). The electrostatic attraction between the negative adsorbent surface and cationic NH_4^+ is beneficial for the adsorption process. However, the percentage of molecular form ammonium nitrogen ($NH_3 \cdot H_2O$) would increase significantly when the pH is larger than 9.0, which limits the cation exchange process of NH_4^+.

3.4. Adsorption isotherms

Fig. 2c compares the adsorption isotherms of NH_4^+ onto LiT, NaT, KT, SrT and BaT (C_0 = 10–160 mg·L^{-1}). It is evident that the equilibrium adsorption capacity of the titanates increases along with the increasing of initial NH_4^+ concentration. In the same environmental conditions, the adsorption performance of titanates for NH_4^+ is in the order of LiT> NaT > KT> > SrT > BaT, which agrees with the results of pH and kinetic experiments.

In order to understand the adsorption process and evaluate the adsorption performance, two typical isotherm models (Langmuir and Freundlich models, Eqs. (S3)–(S4)) have been used to fit the experimental data. The fitting curves are shown in Fig. 2c and the calculated results are listed in Table S2. These curves and the higher value of R^2 demonstrate that Langmuir model is in reasonable agreement with the experimental data, indicating a monolayer NH_4^+ adsorption onto the titanates. The K_L calculated from Langmuir demonstrates that the adsorption of NH_4^+ onto LiT is more favorable than others (Li et al., 2019). Among all the five materials, LiT has the largest calculated adsorption capacity (Q_{max}=50.31 mg·g^{-1}) followed by NaT (44.54 mg·g^{-1}), KT (43.48 mg·g^{-1}), SrT (24.61 mg·g^{-1}) and BaT (24.50 mg·g^{-1}) at the temperature of 25 °C. Table 2 summarizes the adsorption performance of NH_4^+ onto different adsorbents reported in the literature. It is shown that titanates, especially the LiT, possesses an outstanding adsorption performance and fast adsorption rate compared with other commonly used adsorbents such as zeolites and biochar. Finally, the enhancement of adsorption performance by changing counter cation species should be investigated detailedly.

3.5. Cation exchange equilibrium and selectivity

It is evident from the FTIR spectra (Fig. S7) of titanates adsorbent before and adsorption that the peak at about 1340 cm^{-1} corresponding to the Ti—O bond shifts. The peak presents the interaction between Ti—O and exchanged ions. After adsorption, the peak shifts to 1400 cm^{-1} in LiT, NaT and KT, which is attributed to NH_4^+ and indicates that most of the exchangeable ions has been replaced (He et al., 2016). However, there is no peak appearing at about 1400 cm^{-1} and only tiny shift for the Ti—O bond peak occurs during the NH_4^+ adsorption onto SrT or BaT, which demonstrates that cation exchange with Sr^{2+} or Ba^{2+} is difficult.

It is obvious that Li^+, Na^+, K^+, Sr^{2+} and Ba^{2+} exist in the solution after adsorption of NH_4^+ as shown in Fig. 2d. The lower concentration

Table 2
Adsorption characteristics for NH_4^+ by LiT and other reported materials.

Samples	C_0/mg·L^{-1}	Equilibrium time/min	Q_{max}/ mg·g^{-1}	Reference
D113 resin	20–200	30	26.2	(Chen et al., 2015)
Maple wood biochar	0–100	960	5.44	(Wang et al., 2015)
Modified corncob biochar	10–100	120	22.6	(Vu et al., 2017)
Iranian zeolite	90–3610	60	11.5	(Malekian et al., 2011)
natural Chinese (Chende) zeolite	50–300	180	9.41	(Alshameri et al., 2014b)
Na-Yemeni natural zeolite	10–250	20	11.2	(Alshameri et al., 2014a)
NaOH-activated and La-zeolite	20–500	1440	23.9	(He et al., 2016)
Mg-biochar	15–200	1440	51.5	(Xu et al., 2018)
Vermiculite	10–1500	30	50.1	(Alshameri et al., 2018)
Modified bentonite	0–350	60	5.85	(Cheng et al., 2019)
Waste-based biochar	5–150	1500	7.18	(Xue et al., 2019)
Lithium titanate	10–160	10	50.3	This study

C_0 is the initial concentration of adsorbates (NH_4^+ in this report); Equilibrium time is the time needed to reach the adsorption equilibrium; Q_{max} (mg·g^{-1}) is the maximum monolayer molecular adsorption capacity calculated by Langmuir model.

of Sr^{2+} and Ba^{2+} in solution is consistent with the result of Fig. S7. The cation exchange capacity of titanates are calculated according to the concentration of exchanged cations in solution and can present the total cation exchange capacity. The amount of counter cations entering into solution is more than the reduction of NH_4^+ during adsorption process, which might be attributed to that some of counter cations are exchanged by H^+. All the above results indicate that LiT, NaT and KT can successfully exchange with NH_4^+ in the solution. On the contrary, the interactions between Sr^{2+} or Ba^{2+} and titanate framework might be too strong and reject cation exchange with NH_4^+. The difference between monovalent ion and divalent ion might answer for this phenomenon. The divalent ions can enter into the metastable framework of titanates more tightly than monovalent ones due to the possible structure collapse and charge balance (He et al., 2017), which would result in the low exchangeability of SrT and BaT for monovalent NH_4^+.

In order to reveal the effect of counter ions on NH_4^+ removal during cation exchange process in detail, a series of competitive adsorption experiments between NH_4^+ and other co-existing cations were conducted. LiT was chosen as the adsorbent because of its excellent performance for NH_4^+.

The adsorption capacities of LiT for different metal cations with the existence of NH_4^+ are shown in Fig. 3. The competition between individual cation and NH_4^+ varies along with the ion species, and the adsorption capacities of LiT for these ions also differs with each other. It's shown that most cations used here like Sr^{2+} or Ba^{2+} enters into the adsorbent framework in preference to NH_4^+, which is consistent with the phenomenon that NH_4^+ adsorption from water is affected by the co-existing

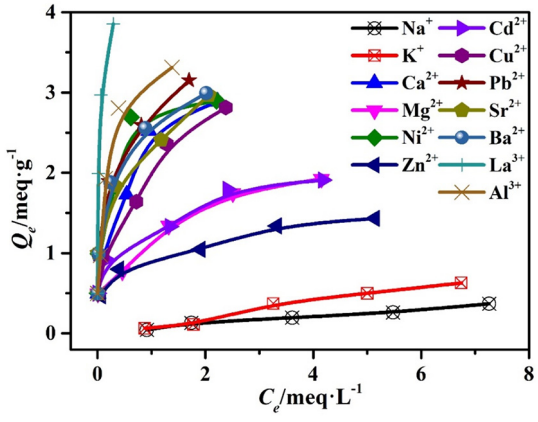

Fig. 3. The ion exchange capacity of different cations onto LiT in the coexistence of NH_4^+. Experimental conditions: initial NH_4^+ concentration 4 meq·L^{-1}, initial cation concentration (like Na^+ or Ca^{2+}) 1.0, 2.0, 4.0, 6.0 and 8.0 meq·L^{-1}, contact time 120 min, initial solution pH 3.5.

cation as shown in literatures (Chen et al., 2018; Guaya et al., 2015). The ion exchange ability with cations are in the order of trivalent ions> divalent ions> monovalent ions, which indicates that the ions valence state affects the ion exchange ability. The above results demonstrate that ion selectivity occurs in the ion exchange with different cations by titanates.

The ion exchange equilibrium is focused to understand the cation selectivity during the ion exchange process for titanates. There are some classical theories or models of ion exchange equilibrium to help understand the ion exchange selectivity (Gaines and Thomas, 1953; Thomas, 1944). Some theories are raised by means of rigorous and abstract thermodynamics, which are correct but only yields a limited information about the physical phenomenon (Helfferich, 1962). Among these models, Donnan equilibrium (Tian et al., 2015) is one of the fundamental theories about ion exchange equilibrium and describes fixed and counter ions partitioning in a quantitative way (Münchinger and Kreuer, 2019; Yang and Wang, 2019).

According to Donnan theory, the selectivity coefficient of cation A to cation B (K_B^A) in the exchange system can be obtained by Eq. (4). Where γ_A or γ_B is activity coefficient of A or B ion, z_A or z_B is charge number of A or B, Π is the swelling pressure, ν_A or ν_B (L·mol^{-1}) is partial molal volume of A or B ion, m_A or m_B (mol·g^{-1}) is molality of A or B ion, R is gas constant (J·(mol·K)$^{-1}$) and T (K) is Kelvin temperature. While the parameter with overbar (such as $\overline{m_A}$) represents the state in framework case (Helfferich, 1962). The first item on the right side of Eq. (4) reflects the interaction between counter cations and fixed anions in framework. The second one reflects the interaction between counter ions and other components in solution (Helfferich, 1962). In this study, the species and concentration of counter ions are the variables, and ion exchange process takes place mainly in the titanate framework. Therefore, the effect of the first item on the value of K_B^A is more remarkable compared to the second item. In addition, the third item can be ignored because the swelling pressure Π of inorganic materials is usually very low like titanates in this study. Therefore, the discussion of selectivity coefficient can be simplified to only the first item on Eq. (4), i.e. the interaction between counter cations and fixed anions in the framework.

$$\ln K_B^A = \ln \frac{\overline{m}_A{}^{z_B} m_B{}^{z_A}}{\overline{m}_B{}^{z_A} m_A{}^{z_B}} = \ln \frac{\overline{\gamma_B}^{z_A}}{\overline{\gamma_A}^{z_B}} + \ln \frac{\gamma_A{}^{z_B}}{\gamma_B{}^{z_A}} + \frac{\Pi}{RT}(z_A\nu_B - z_B\nu_A) \quad (4)$$

Usually the electrostatic attraction is the main or common interaction between cations and anions among other interactions like ion pairs and covalent bonds. It is also the same case for interaction between counter cations and fixed anions in the frame work. The electrostatic attraction between counter ions and charged framework is dependent on charge number and average minimum distance which is related to Debye-Huckel parameter (Celebi et al., 2019).The effect of ion properties like valence, ion radius and hardness on ion exchange selectivity

Table 3
The values of valence and hydrated radius of some common cations.

Cations	Valence	r_A[a]/Å
Li^+	+1	3.82
Na^+	+1	3.58
K^+	+1	3.31
NH_4^+	+1	3.31
Mg^{2+}	+2	4.28
Ca^{2+}	+2	4.12
Zn^{2+}	+2	4.30
Cd^{2+}	+2	4.26
Cu^{2+}	+2	4.19
Ni^{2+}	+2	4.04
Sr^{2+}	+2	4.12
Ba^{2+}	+2	4.04
Pb^{2+}	+2	4.01
Al^{3+}	+3	4.75
La^{3+}	+3	4.52

[a] The data of cation hydrated radius (r_A) is given by Nightingale (Nightingale, 1959).

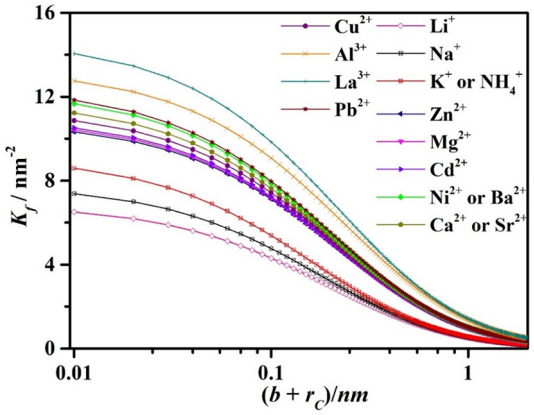

Fig. 4. The values of affinity coefficient to titanates for different counter cations obtained by Eq. (5).

have been qualitative discussed before (He et al., 2017; Li et al., 2012; Mubita et al., 2019). However, the qualitative discussion is not precise when there are more than one parameter taking effects oppositely. For instance, the effects of ion radius and valence on selectivity are opposite and these two parameters of Na^+ are different from that of Ca^{2+} in value, which might easily make confusion. It is essential to establish a brief but direct relation between cations properties and ion selectivity or affinity.

The values of ion valence and hydrated radius of cations used in the competitive experiments are listed in Table 3 (Nightingale, 1959; Shannon, 1976). According to the results of Fig. 3 and Table 3, the higher valence or the smaller hydrated radius corresponds to the higher affinity of cations to titanate framework in general, which is consistent with results in literatures (Li et al., 2012). Considering that the electrostatic interaction between counter ions and fixed ions (in framework) plays a key role in the motion of counter ions, the Coulomb's law is referenced here to explain the affinity or selectivity order of the cations. The affinity coefficient K_f of cation A to titanates is defined and used instead of K_B^A for direct prediction by Eq. (5) ($K_B^A = \frac{K_f^A}{K_f^B}$), where z_A is the valence of cation A, r_A is the hydration radius of counter ion A, r_C is the hydration radius of fixed ion C and is thought to be constant for different case in this study, b is the distance between fixed ions and hydrated counter ions. Supposing that the value of b is constant for different counter ions when other conditions are consistent, the results of K_f can be calculated as shown in Fig. 4.

$$K_f = \frac{z_A}{(b + r_A + r_C)^2} \tag{5}$$

It is notable that the results of Fig. 4 from Eq. (5) can successfully explain the affinity or selectivity of most common cations to titanates when compared to the results of competitive experiment (Fig. 3). The good agreement demonstrates that the valence and hydrated radius of cations conversely affect the cation exchange selectivity in the light of Eq. (5). The higher K_f value of cation, the higher selectivity or affinity of cation to titanates. The results show that the K_f values of NH_4^+, Li^+, Na^+, K^+, Sr^{2+} and Ba^{2+} are in the order of $Ba^{2+} > Sr^{2+} > > K^+ = NH_4^+ > Na^+ > Li^+$, which demonstrates that Li^+, Na^+ and K^+ can be exchanged out from titanate framework more easily and completely than Sr^{2+} or Ba^{2+} when NH_4^+ is in external solution. Therefore, the definition of K_f successfully reveals the main reason about the effect of counter ion species on the adsorption of NH_4^+ from water by titanates and can also help explain the enhancement of adsorption performance of LT for NH_4^+. The results and findings discussed above are combined in a diagram as shown in Fig. 5. Furthermore, the definition and discussion can also be used for future ion exchange mechanism analysis and

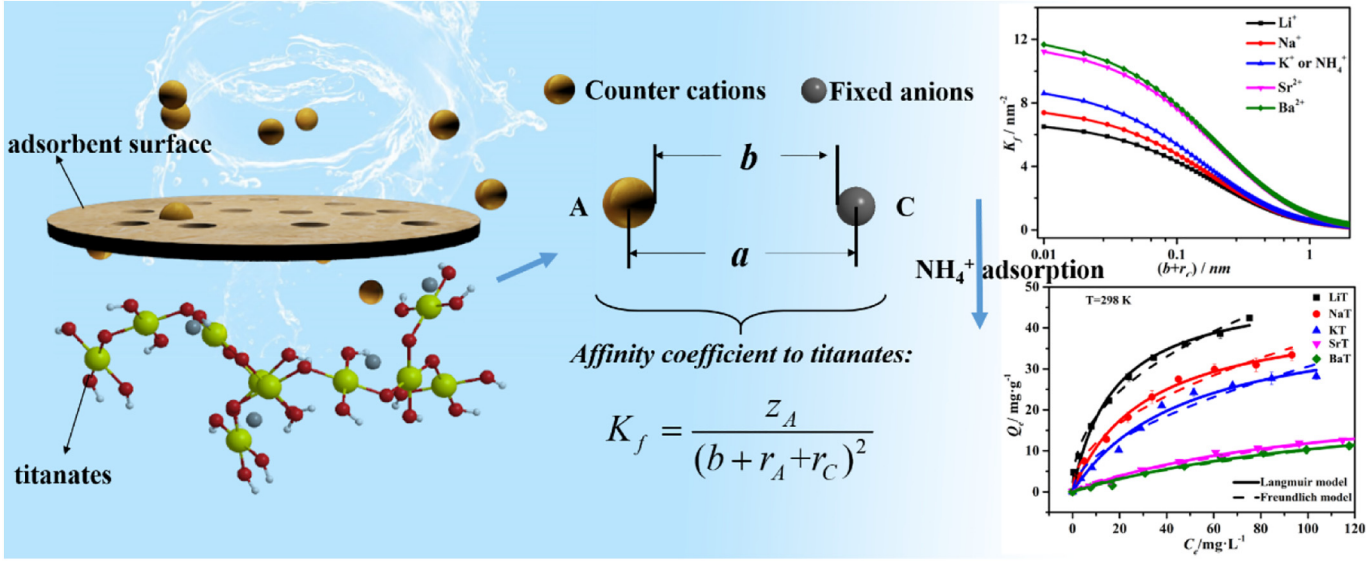

Fig. 5. The effect of counter cations species on ion exchange equilibrium.

adsorbent design especially for the inorganic ion-exchanger because the definition of K_f value is brief and effective.

4. Conclusions

In this study, the cation exchange for NH_4^+ uptake is focused on to enhance the adsorption capacity for titanates. A series of titanates (LiT, NaT, KT, SrT, BaT) containing different counter cations were synthesized and served as adsorbents for the uptake of NH_4^+ from aqueous solution. The primary conclusions according to the experimental results and discussion are as follows:

The adsorption capacity of titanates for NH_4^+ is in the order of LiT> NaT > KT> > SrT > BaT, which is regulated by changing counter cations in framework of adsorbents. The adsorption capacity of LiT is as high as 50.31 $mg \cdot g^{-1}$, which is about 5 times larger than that of BaT. The adsorption equilibrium of NH_4^+ onto titanates can be reached quickly within 10 min. A brief but effective parameter affinity coefficient K_f is introduced and can satisfactorily reveal that the valence and hydrated radius have opposite effect on ion selectivity of counter ions to titanates. The inorganic nature and manageable structure-function relationship make titanate a stable and efficient adsorbent for NH_4^+ removal.

CRediT authorship contribution statement

Wenlong Zhang: Conceptualization, Methodology, Formal analysis, Investigation, Writing – original draft. **Zhenyu Wang:** Software, Visualization. **Yunpeng Liu:** Validation, Investigation. **Jiangtao Feng:** Resources, Data curation, Writing – review & editing, Funding acquisition. **Jie Han:** Writing – review & editing. **Wei Yan:** Resources, Supervision, Project administration, Funding acquisition.

Declaration of competing interest

The authors declare that they have no known competing financial interests or personal relationships that could have appeared to influence the work reported in this paper.

Acknowledgements

This research is supported by National Natural Science Foundation of China (Grant No.51978569), Research Fund for Young Talent Support Plans of Xi'an Jiaotong University, the Shaanxi Key Research and Development Projects, China (Grant No. 2017SF-386), and the Fundamental Research Funds for the Central Universities of China.

Appendix A. Supplementary data

Supplementary data to this article can be found online at https://doi.org/10.1016/j.scitotenv.2020.144800.

References

Abukhadra, M.R., Mostafa, M., 2019. Effective decontamination of phosphate and ammonium utilizing novel muscovite/phillipsite composite; equilibrium investigation and realistic application. Sci. Total Environ. 667, 101–111.

Adam, M.R., Matsuura, T., Othman, M.H.D., Puteh, M.H., Pauzan, M.A.B., Ismail, A.F., et al., 2019a. Feasibility study of the hybrid adsorptive hollow fibre ceramic membrane (HFCM) derived from natural zeolite for the removal of ammonia in wastewater. Process. Saf. Environ. Prot. 122, 378–385.

Adam, M.R., Othman, M.H.D., Abu, Samah R., Puteh, M.H., Ismail, A.F., Mustafa, A., et al., 2019b. Current trends and future prospects of ammonia removal in wastewater: a comprehensive review on adsorptive membrane development. Sep. Purif. Technol. 213, 114–132.

Alshameri, A., Ibrahim, A., Assabri, A.M., Lei, X.R., Wang, H.Q., Yan, C.J., 2014a. The investigation into the ammonium removal performance of Yemeni natural zeolite: modification, ion exchange mechanism, and thermodynamics. Powder Technol. 258, 20–31.

Alshameri, A., Yan, C.J., Al, Ani Y., Dawood, A.S., Ibrahim, A., Zhou, C.Y., et al., 2014b. An investigation into the adsorption removal of ammonium by salt activated Chinese (Hulaodu) natural zeolite: kinetics, isotherms, and thermodynamics. J. Taiwan Inst. Chem. Eng. 45, 554–564.

Alshameri, A., He, H.P., Zhu, J.X., Xi, Y.F., Zhu, R.L., Ma, L.Y., et al., 2018. Adsorption of ammonium by different natural clay minerals: characterization, kinetics and adsorption isotherms. Appl. Clay Sci. 159, 83–93.

Celebi, A.T., Cetin, B., Beskok, A., 2019. Molecular and continuum perspectives on intermediate and flow reversal regimes in electroosmotic transport. J. Phys. Chem. C 123, 14024–14035.

Chen, Y.C., Lo, S.L., Kuo, J., 2010. Pb(II) adsorption capacity and behavior of titanate nanotubes made by microwave hydrothermal method. Colloids Surf. A Physicochem. Eng. Asp. 361, 126–131.

Chen, Y.N., Luo, X.Y., Xiong, C.S., Liang, L.M., 2015. The mechanism of ion exchange and adsorption coexist on medium-low concentration ammonium-nitrogen removal by ion-exchange resin. Environ. Technol. 36, 2349–2356.

Chen, H.F., Lin, Y.J., Chen, B.H., Yoshiyuki, I., Liou, S., Huang, R.T., 2018. A further investigation of NH_4^+ removal mechanisms by using natural and synthetic zeolites in different concentrations and temperatures. Minerals 8, 499–511.

Chen, Y., Chen, W., Chen, Q.Z., Peng, C.H., He, D.W., Zhou, K.G., 2019. Removal of ammonia-nitrogen in wastewater using a novel poly ligand exchanger-Zn(II)-loaded chelating resin. Water Sci. Technol. 79, 126–136.

Cheng, H.M., Zhu, Q., Xing, Z.P., 2019. Adsorption of ammonia nitrogen in low temperature domestic wastewater by modification bentonite. J. Clean. Prod. 233, 720–730.

di Bitonto, L., Volpe, A., Pagano, M., Bagnuolo, G., Mascolo, G., La Parola, V., et al., 2017. Amorphous boron-doped sodium titanates hydrates: efficient and reusable adsorbents for the removal of Pb^{2+} from water. J. Hazard. Mater. 324, 168–177.

Gaines, G.L., Thomas, H.C., 1953. Adsorption studies on clay minerals. II. A formulation of the thermodynamics of exchange adsorption. J. Chem. Phys. 21, 714–718.

Guaya, D., Valderrama, C., Farran, A., Armijos, C., Cortina, J.L., 2015. Simultaneous phosphate and ammonium removal from aqueous solution by a hydrated aluminum oxide modified natural zeolite. Chem. Eng. J. 271, 204–213.

He, Y.H., Lin, H., Dong, Y.B., Liu, Q.L., Wang, L., 2016. Simultaneous removal of ammonium and phosphate by alkaline-activated and lanthanum-impregnated zeolite. Chemosphere 164, 387–395.

He, W.Y., Ai, K.L., Ren, X.Y., Wang, S.Y., Lu, L.H., 2017. Inorganic layered ion-exchangers for decontamination of toxic metal ions in aquatic systems. J. Mater. Chem. A 5, 19593–19606.

Helfferich, F.G., 1962. Ion Exchange. McGraw-Hill, New York.

Hu, R., Xiao, J., Wang, T.H., Chen, G.C., Chen, L., Tian, X.Y., 2020. Engineering of phosphate-functionalized biochars with highly developed surface area and porosity for efficient and selective extraction of uranium. Chem. Eng. J. 379, 122388.

Huang, L., Li, L., Dong, W.B., Liu, Y., Hou, H.Q., 2008. Removal of ammonia by OH radical in aqueous phase. Environ. Sci. Technol. 42, 8070–8075.

Kamcev, J., Galizia, M., Benedetti, F.M., Jang, E.S., Paul, D.R., Freeman, B.D., et al., 2016. Partitioning of mobile ions between ion exchange polymers and aqueous salt solutions: importance of counter-ion condensation. Phys. Chem. Chem. Phys. 18, 6021–6031.

Kamcev, J., Paul, D.R., Manning, G.S., Freeman, B.D., 2017. Accounting for frame of reference and thermodynamic non-idealities when calculating salt diffusion coefficients in ion exchange membranes. J. Membr. Sci. 537, 396–406.

Katchalsky, A., Lifson, S., Mazur, J., 1953. The electrostatic free energy of polyelectrolyte solutions. I. Randomly kinked macromolecules. J. Polym. Sci. 11, 409–423.

Kelly, P.T., He, Z., 2014. Nutrients removal and recovery in bioelectrochemical systems: a review. Bioresour. Technol. 153, 351–360.

Khollam, Y.B., Deshpande, S.B., Potdar, H.S., Bhoraskar, S.V., Sainkar, S.R., Date, S.K., 2005. Simple oxalate precursor route for the preparation of barium–strontium titanate: $Ba_{1-x}Sr_xTiO_3$ powders. Mater. Charact. 54, 63–74.

Lazare, L., Sundheim, B.R., Gregor, H.P., 1956. A model for cross-linked polyelectrolytes. J. Phys. Chem. 60, 641–648.

Li, N., Zhang, L.D., Chen, Y.Z., Fang, M., Zhang, J.X., Wang, H.M., 2012. Highly efficient, irreversible and selective ion exchange property of layered titanate nanostructures. Adv. Funct. Mater. 22, 835–841.

Li, J., Zhang, Q., Feng, J., Yan, W., 2013. Synthesis of PPy-modified TiO_2 composite in H_2SO_4 solution and its novel adsorption characteristics for organic dyes. Chem. Eng. J. 225, 766–775.

Li, M.X., Liu, H.B., Chen, T.H., Dong, C., Sun, Y.B., 2019. Synthesis of magnetic biochar composites for enhanced uranium(VI) adsorption. Sci. Total Environ. 651, 1020–1028.

Malekian, R., Abedi-Koupai, J., Eslamian, S.S., Mousavi, S.F., Abbaspour, K.C., Afyuni, M., 2011. Ion-exchange process for ammonium removal and release using natural Iranian zeolite. Appl. Clay Sci. 51, 323–329.

Mubita, T.M., Dykstra, J.E., Biesheuvel, P.M., van der Wal, A., Porada, S., 2019. Selective adsorption of nitrate over chloride in microporous carbons. Water Res. 164, 114885.

Münchinger, A., Kreuer, K.-D., 2019. Selective ion transport through hydrated cation and anion exchange membranes I. The effect of specific interactions. J. Membr. Sci. 592, 117372.

Nightingale, E.R., 1959. Phenomenological theory of ion solvation. Effective radii of hydrated ions. J. Phys. Chem. 63, 1381–1387.

O'Connor, E., Kavanagh, O.N., Chovan, D., Madden, D.G., Cronin, P., Albadarin, A.B., et al., 2020. Highly selective trace ammonium removal from dairy wastewater streams by aluminosilicate materials. J. Ind. Eng. Chem. 86, 39–46.

Sadeghzadeh, Attar A., Salehi, Sichani E., Sharafi, S., 2017. Structural and dielectric properties of bi-doped barium strontium titanate nanopowders synthesized by sol–gel method. J. Mater. Res. Technol. 6, 108–115.

Shannon, R.D., 1976. Revised effective ionic radii and systematic studies of interatomic distances in halides and chalcogenides. Acta Cryst 32, 751–767.

Thomas, H.C., 1944. Heterogeneous ion exchange in a flowing system. J. Am. Chem. Soc. 66, 1664–1666.

Tian, H., Zhang, L., Wang, M., 2015. Applicability of Donnan equilibrium theory at nanochannel-reservoir interfaces. J. Colloid Interface Sci. 452, 78–88.
Vocciante, M., De Folly D'Auris, A., Finocchi, A., Tagliabue, M., Bellettato, M., Ferrucci, A., et al., 2018. Adsorption of ammonium on clinoptilolite in presence of competing cations: investigation on groundwater remediation. J. Clean. Prod. 198, 480–487.
Vu, T.M., Trinh, V.T., Doan, D.P., Van, H.T., Nguyen, T.V., Vigneswaran, S., et al., 2017. Removing ammonium from water using modified corncob-biochar. Sci. Total Environ. 579, 612–619.
Wang, B., Lehmann, J., Hanley, K., Hestrin, R., Enders, A., 2015. Adsorption and desorption of ammonium by maple wood biochar as a function of oxidation and pH. Chemosphere 138, 120–126.
Wang, Q.R., Zheng, C.L., Shen, Z.X., Lu, Q., He, C., Zhang, T.C., et al., 2019. Polyethyleneimine and carbon disulfide co-modified alkaline lignin for removal of Pb^{2+} ions from water. Chem. Eng. J. 359, 265–274.
Xu, K.N., Lin, F.Y., Dou, X.M., Zheng, M., Tan, W., Wang, C.W., 2018. Recovery of ammonium and phosphate from urine as value-added fertilizer using wood waste biochar loaded with magnesium oxides. J. Clean. Prod. 187, 205–214.
Xue, S., Zhang, X.B., Ngo, H.H., Guo, W.S., Wen, H.T., Li, C.C., et al., 2019. Food waste based biochars for ammonia nitrogen removal from aqueous solutions. Bioresour. Technol. 292, 121927.
Yang, Y.K., Wang, M.R., 2019. Cation diffusion in compacted clay: a pore-scale view. Environ. Sci. Technol. 53, 1976–1984.
Yang, D.J., Liu, H.W., Zheng, Z.F., Sarinab, S., Zhu, H.Y., 2013. Titanate based adsorbents for radioactive ions entrapment from water. Nanoscale 5, 2232–2242.
Yang, X.Y., Liu, Q., Fu, G.T., He, Y., Luo, X.Z., Zheng, Z., 2016. Spatiotemporal patterns and source attribution of nitrogen load in a river basin with complex pollution sources. Water Res. 94, 187–199.
Ye, M.M., Lu, Z.D., Hu, Y.X., Zhang, Q., Yin, Y.D., 2013. Mesoporous titanate based cation exchanger for efficient removal of metal cations. J. Mater. Chem. A 1, 5097–5104.
Zhang, L., Zhang, Q.H., Xie, H.Y., Guo, J., Lyu, H.L., Li, Y.G., et al., 2017. Electrospun titania nanofibers segregated by graphene oxide for improved visible light photocatalysis. Appl. Catal., B 201, 470–478.
Zhang, W., Fu, R., Wang, L., Zhu, J., Feng, J., Yan, W., 2019. Rapid removal of ammonia nitrogen in low-concentration from wastewater by amorphous sodium titanate nanoparticles. Sci. Total Environ. 668, 815–824.
Zhao, T.H., Tang, Z., Zhao, X.L., Zhang, H., Wang, J.Y., Wu, F.C., et al., 2019. Efficient removal of both antimonite (Sb(iii)) and antimonate (Sb(v)) from environmental water using titanate nanotubes and nanoparticles. Environ. Sci. Nano 6, 834–850.
Zheng, Y.A., Wang, A.Q., 2015. Superadsorbent with three-dimensional networks: from bulk hydrogel to granular hydrogel. Eur. Polym. J. 72, 661–686.